Available online at www.sciencedirect.com
ScienceDirect
Journal of the European Ceramic Society 26 (2006) 3173–3179
www.elsevier.com/locate/jeurceramsoc

Electrically conductive ZrO_2–TiN composites

Sedigheh Salehi, Omer Van der Biest, Jef Vleugels *

Department of Metallurgy and Materials Engineering, Katholieke Universiteit Leuven, Kasteelpark Arenberg 44, B-3001 Heverlee, Belgium

Received 3 September 2005; accepted 29 October 2005
Available online 13 December 2005

Abstract

1.75 mol% Y_2O_3-stabilized ZrO_2–TiN composites could be fully densified by hot pressing for 1 h at 1550 °C in vacuum under a mechanical pressure of 28 MPa. Composites with 35–95 vol% TiN were investigated and the best mechanical properties, i.e., a Vickers hardness of 14.7 GPa, an indentation toughness of 5.9 MPa $m^{1/2}$ and an excellent bending strength of 1674 MPa were obtained with 40 vol% TiN. The active toughening mechanisms were identified and their contribution to the overall composite toughness as function of the TiN content was modelled, experimentally verified and discussed. Transformation toughening was found to be the primary toughening mechanism. The TiN grain size was found to increase with increasing TiN content, resulting in a decreasing hardness and strength. A maximum strength was obtained at 40 vol% TiN. The electrical resistivity of the composites decreases exponentially with increasing TiN content and correlates well with the Polder-Van Santen mixture rule. Thus at around 40 vol% TiN, the conductivity is high enough to allow EDM machining of the composite, therefore avoiding the expensive grinding operation for final shaping and surface finishing of components.

Keywords: Composites; Mechanical properties; Toughness; ZrO_2; TiN; EDM; Electrical conductivity

1. Introduction

During the last decade, the applicability of zirconia to induce toughening by the stress-induced transformation of the tetragonal to monoclinic ZrO_2 phase in the stress field of propagating cracks, a phenomenon known as transformation toughening,[1,2] has been intensively investigated. Recent developments in zirconia composites are focused not only on the improvement of toughness, strength and hardness, but also on the possibility for mass production and manufacturing cost reduction. A successful approach is to incorporate electrically conductive reinforcements such as TiB_2,[3] WC,[4] ZrB_2,[5] TiC,[6] TiCN[6] and TiN into the zirconia matrix. The incorporation of a certain content of these conductive reinforcements makes the composite electrically conductive enough to be machineable by electrical discharge machining (EDM), thus avoiding the expensive grinding operation for final shaping and surface finishing of components. Electrical resistivity threshold values for EDM are reported to be in between 100 and 300 Ω cm.[7,8]

To the best of the authors' knowledge however, no in depth study has been reported on ZrO_2–TiN composites with a TiN content ranging from 35–95 vol%. The goal of the present work is to investigate and evaluate the mechanical properties and electrical conductivity of ZrO_2–TiN composites with a TiN phase content in this range.

2. Experimental procedure

Yttria-stabilized ZrO_2–TiN composites with 35–95 vol% TiN and 0.75 wt.% Al_2O_3 were investigated. Details on the commercial starting powders are given in Table 1. The commercial powders are yttria-free monoclinic ZrO_2 (Tosoh grade TZ-0, Tokyo, Japan), 3 mol% yttria co-precipitated ZrO_2 (Tosoh grade TZ-3Y, Tokyo, Japan) and jet-milled TiN (Kennametal, Victoria, USA). The Y_2O_3-stabiliser content of the powder mixtures was adjusted by mixing the appropriate ratio of ZrO_2 starting powders. 0.75 wt.% Al_2O_3 powder (Baikowski grade SM8, Annecy, France) was added as a ZrO_2 grain growth inhibitor and sintering aid to all composite grades.

Fifty grams of fully formulated powder mixture was mixed on a multidirectional Turbula mixer (type T2A, Basel, Switzerland) in ethanol in a polyethylene container of 250 ml during 24 h

* Corresponding author. Tel.: +32 16 32 12 44; fax: +32 16 32 19 92.
E-mail address: Jozef.Vleugels@mtm.kuleuven.be (J. Vleugels).

0955-2219/$ – see front matter © 2005 Elsevier Ltd. All rights reserved.
doi:10.1016/j.jeurceramsoc.2005.10.010

Table 1
Starting powders

Powder	Grade	Supplier	Crystal size[a]
ZrO_2	TZ-0	Tosoh (Japan)	27 nm
ZrO_2	TZ-3Y	Tosoh (Japan)	27 nm
TiN	Jet-milled	Kennametal (USA)	1.03 μm
Al_2O_3	SM8	Baikowski (France)	0.60 μm

[a] According to the supplier datasheets.

at 60 rpm. Two hundred and fifty grams zirconia milling balls (Tosoh grade TZ-3Y, Tokyo, Japan) with a diameter of 3 mm were added to the container to break the agglomerates in the starting powder and to enhance powder mixing. The ethanol was removed after mixing using a rotating evaporator.

The dry powder mixture was inserted into a graphite die/punch set-up (diameter of 43 mm), manually coated with boron nitride to avoid carbon diffusion and sample-die sticking. After cold compression at 30 MPa, the samples were hot pressed (Model W100/150-2200-50 LAX, FCT Systeme, Rauenstein, Germany) in vacuum (∼0.1 Pa) for 1 h under a mechanical load of 28 MPa at 1550 °C, with a heating rate of 50 °C/min and a cooling rate of 10 °C/min.

The density of the samples was measured in ethanol, according to the Archimedes method (BP210S balance, Sartorius AG, Germany). The Vickers hardness (HV_{10}) was measured on a Zwick hardness tester (model 3202, Zwick, Ulm, Germany) with an indentation load of 10 kg. The indentation toughness, K_{IC}, based on the crack length measurement of the radial crack pattern produced by Vickers HV_{10} indentations, was calculated according to the formula of Anstis et al.[9] The reported hardness and toughness values are the mean with standard deviation obtained from five indentations.

The elastic modulus (E) of the ceramic specimens was measured using the resonance frequency method.[10] The resonance frequency was measured by the impulse excitation technique (Model Grindo-Sonic, J. W. Lemmens N.V., Leuven, Belgium). The reported values are the mean and standard deviation of 10 measurements.

The flexural strength at room temperature was measured in a 3-point bending test (Instron 4467, PA, USA) on rectangular samples (25.0 mm × 5.4 mm × 2.1 mm), with a span length of 20 mm and a cross-head displacement of 0.1 mm/min. The reported values are the mean with standard deviation of five measurements. All sample surfaces were ground with a diamond grinding wheel (type MD4075B55, Wendt Boart, Brussels, Belgium) on a Jung grinding machine (JF415DS, Göppingen, Germany).

Microstructural investigation was performed by scanning electron microscopy (SEM, XL-30FEG, FEI, Eindhoven, The Netherlands). X-ray diffraction (Seifert 3003 T/T, Ahrensburg, Germany) analysis was used for phase identification and calculation of the relative phase content of monoclinic and tetragonal ZrO_2.

The electrical resistance of the samples was measured according to the 4-point contact method using a Resistomat (TYP 2302 Burster, Gernsbach, Germany).

3. Results and discussion

3.1. Microstructures

The microstructures of polished cross-sectioned ceramics are presented as function of the TiN content in Fig. 1. Three phases can be distinguished, i.e., yttria-stabilized ZrO_2 (bright), TiN (grey) and Al_2O_3 (black). The microstructural investigation of the samples revealed that all samples were fully densified since no pores were found on the cross-sections and the measured density of the composites is 99–100% of the theoretical density, calculated using a theoretical density for ZrO_2, TiN and Al_2O_3 of 6.05, 5.43 and 2.90 g/cm^3, respectively. Moreover, homogeneous ZrO_2–TiN–Al_2O_3 microstructures were obtained, indicating that the powder mixing procedure was appropriate. The composite with 35 vol% TiN has the smallest TiN grain size, which is found to increase with increasing TiN content.

The X-ray diffraction patterns in the 2θ range from 25° to 40° of the polished yttria-stabilized ZrO_2–TiN–Al_2O_3 composites with varying TiN content are shown in Fig. 2, revealing that no monoclinic zirconia phase is present in all investigated composites. This means that no spontaneous martensitic transformation occurred in the composites during cooling from the sintering temperature. Therefore, 1.75 mol% yttria is sufficient enough to stabilize the tetragonal ZrO_2 phase in the ZrO_2–TiN–Al_2O_3 composites with up to 95 vol% TiN.

3.2. Mechanical properties

In order to find the optimum yttria stabilizer content, the yttria content in ZrO_2-based composites with 40 vol% TiN and 0.75 wt.% Al_2O_3 was varied from 2.5 down to 1.0 mol%. The resulting hardness and fracture toughness of the hot pressed composites is graphically presented in Fig. 3. The fracture toughness increases with increasing yttria content up to a maximum of 7 MPa m$^{1/2}$ at 1.75 mol% Y_2O_3 and decreases again upon addition of more stabilizer. This is completely in agreement with the toughness evolution of monolithic ZrO_2 since the transformability and concomitant transformation toughness increases with decreasing yttria content, resulting in spontaneous transformation at too low stabilizer contents. The spontaneous transformation of the ZrO_2 phase is accompanied by microcracking, explaining the reduced hardness at yttria contents below 1.6 mol%. Because of the optimum toughness in combination with maximum hardness, an yttria content of 1.75 mol% was selected to investigate the influence of the TiN content.

The mechanical properties of the 1.75 mol% Y_2O_3-stabilised ZrO_2 with varying TiN content and 0.75 wt.% Al_2O_3 are summarized in Table 2.

A comparison between the measured elastic modulus and the theoretically calculated values is shown in Fig. 4. Calculations were done based on the Voigt[11] and Reuss[12] models using an elastic modulus of 471 GPa for TiN[13] and 200 GPa for stabilized ZrO_2,[14] revealing that the experimental values fall in-between the upper Voigt (*iso*-strain) and lower Reuss (*iso*-stress) boundaries.

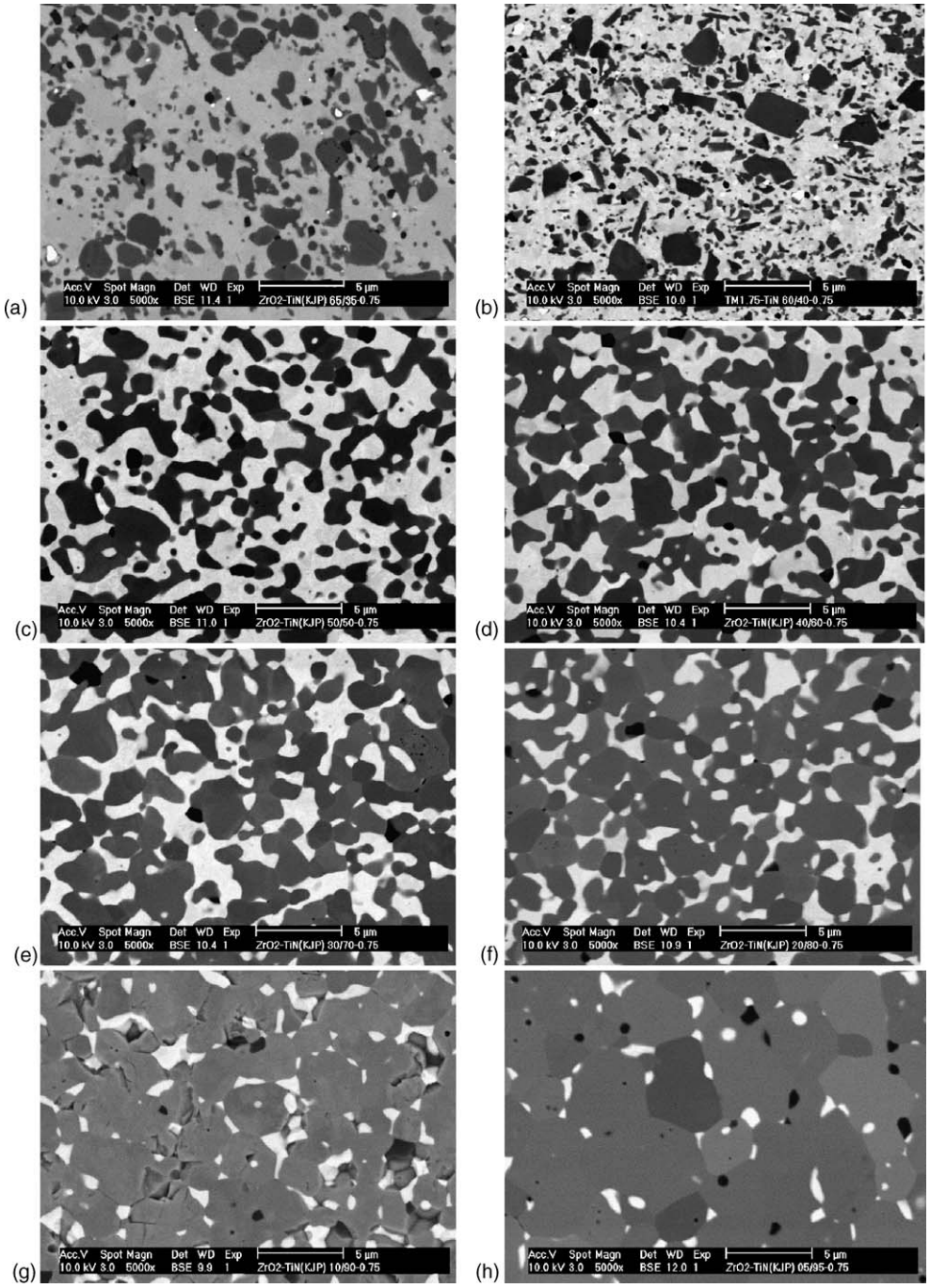

Fig. 1. Backscattered SEM micrographs of polished 1.75 mol% yttria-stabilized ZrO_2–TiN–Al_2O_3 composites with 35 (a), 40 (b), 50 (c), 60 (d), 70 (e), 80 (f), 90 (g) and 95 (h) vol% TiN and 0.75 wt.% Al_2O_3. Three phases can be differentiated; ZrO_2: bright, TiN: grey and Al_2O_3: black.

The Vickers hardness of the composites decreases with decreasing ZrO_2 content, as graphically presented in Fig. 5, what can be attributed to an increasing TiN grain size with increasing TiN content. The bending strength shows an optimum around 40 vol% TiN addition, considering that the strength of pure yttria-stabilized zirconia hot pressed at 1450 °C is about 950 MPa.[6] The decrease in bending strength at higher TiN contents can also be attributed to the increasing TiN grain size.

The contribution of transformation toughening to the overall fracture toughness of the composite can be calculated from the measured composite transformability, which is calculated from the measured ZrO_2 phase transformability multiplied by the ZrO_2 phase fraction in the composite.[15] The ZrO_2 phase transformability is defined as the difference in the percentage of monoclinic and tetragonal zirconia phase, obtained from XRD patterns of smoothly polished and fractured surfaces. The volume fraction of the *m*-ZrO_2, V_m, is calculated by measuring the intensities of the (1 1 1) and (1 1 $\bar{1}$) reflections of the monoclinic ZrO_2 phase and the (1 1 1) peak of the tetragonal ZrO_2 phase according to the formula of Toraya et al.[15] The *m*-ZrO_2

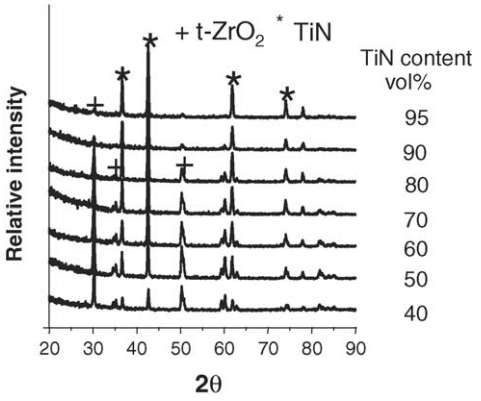

Fig. 2. X-ray diffraction patterns of polished yttria-stabilized ZrO_2–TiN–Al_2O_3 composites with varying TiN content.

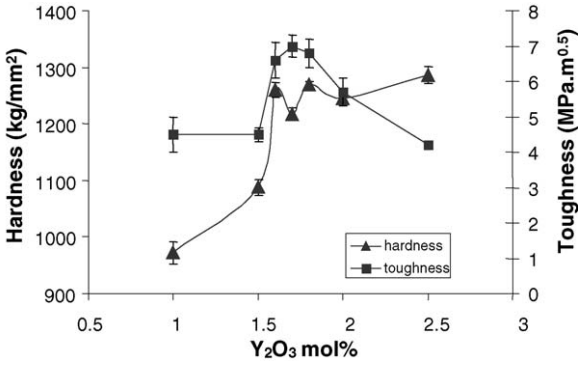

Fig. 3. Hardness and toughness of hot pressed ZrO_2–TiN–Al_2O_3 (60/40/0.75) composites as function of the yttria stabiliser content.

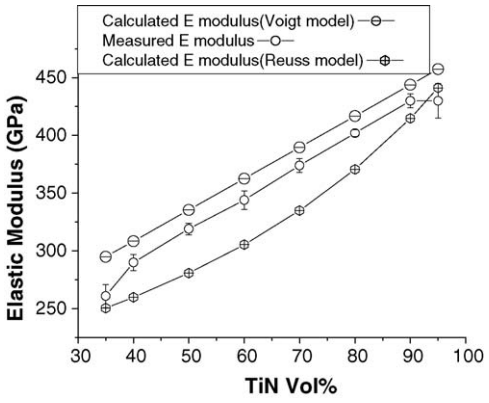

Fig. 4. Measured and calculated E modulus of the yttria-stabilized ZrO_2–TiN–Al_2O_3 composites as function of the TiN content.

fraction measured on the fractured surface, the ZrO_2 phase transformability and the composite transformability are summarized in Table 3, allowing to calculate the actual transformation toughening contribution, assuming that a composite transformability of 63% results in a toughness contribution of 6.6 MPa $m^{1/2}$.[4] Since no m-ZrO_2 was measured on the polished surfaces of all investigated composites, the ZrO_2 phase transformability is equal to the measured m-ZrO_2 content on the fractured surface.

The lower coefficient of thermal expansion of TiN ($\alpha_{0–1000\,^\circ C} = 9.4 \times 10^{-6}/^\circ C$)[16] compared to Yttria-stabilized ZrO_2 ($\alpha_{0–1000\,^\circ C} = 10 \times 10^{-6}/^\circ C$)[14] will cause compressive residual stresses on the TiN phase. This residual compressive stress can provide an extra fracture toughening mechanism on the TiN

Table 2
Mechanical properties of 1.75 mol% Y_2O_3-stabilised ZrO_2–TiN composites with varying TiN content and 0.75 wt.% Al_2O_3

TiN content (vol%)	ρ (g/cm^3)	E (GPa)	HV_{10} (GPa)	K_{IC} (MPa $m^{1/2}$)	3-point bending strength[a] (MPa)	El. resistivity (10^{-6} Ωm)
35	5.85	261 ± 10	13.75 ± 0.08	7.1 ± 0.2	909 ± 140	7.45
40	5.81	290 ± 7	13.65 ± 0.09	5.9 ± 0.1	1674 ± 314	4.60
50	5.69	319 ± 5	13.49 ± 0.26	6.3 ± 0.5	1429 ± 61	1.58
60	5.60	344 ± 8	13.55 ± 0.25	5.0 ± 0.3	1464 ± 66	0.91
70	5.55	374 ± 6	13.63 ± 0.16	4.7 ± 0.2	1268 ± 87	0.60
80	5.49	402 ± 3	13.36 ± 0.08	4.0 ± 0.5	1307 ± 102	0.43
90	5.40	430 ± 6	12.97 ± 0.18	4.8 ± 0.5	916 ± 56	0.38
95	5.39	430 ± 15	12.91 ± 0.29	3.3 ± 0.2	678 ± 81	0.39

[a] Sample size = 45 mm × 4.30 mm (width) × 1.44 mm (height).

Table 3
ZrO_2 phase and composite transformability together with the resulting transformation toughening contribution for yttria-stabilized ZrO_2–TiN–Al_2O_3 composites

TiN (vol%)	m-ZrO_2 content on fractured surface (volume fraction)	Zirconia phase transformability (%)	Composite transformability (%)	ΔK_{IC} (MPa $m^{1/2}$)
35	0.48	48	31	3.31
40	0.40	40	24	2.52
50	0.31	31	15	1.63
60	0.39	39	15	1.66
70	0.24	24	7	0.77
80	0.26	26	5	0.54
90	0.16	16	1	0.17
95	0.20	20	1	0.10

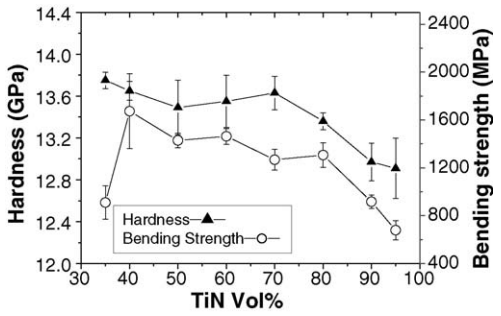

Fig. 5. Vickers hardness and 3-point bending strength for the ZrO_2–TiN–Al_2O_3 composites as function of the TiN content.

phase that can be calculated as[17]:

$$\Delta K_{IC} = 2q\sqrt{\frac{2D}{\pi}}$$

where K_{IC} is the critical stress intensity factor of the matrix, q is the local residual stress, and D is the length of the compressive stress zone, which in this case is the average particulate spacing of the zirconia particles. The local residual stress, q, can be calculated from the overall composite composition and the E modulus of the constituent phases according to the theoretical model proposed by Taya et al.[17] The presence of the Al_2O_3 phase was ignored for these calculations, whereas a Young's modulus of 471 and 200 GPa was used for TiN and ZrO_2, respectively. The ZrO_2 interparticle distance, D, was obtained according to the linear intercept method[18] using IMAGE-PRO software on SEM pictures. The calculated residual stress in the TiN phase, the measured interparticle distance and the concomitant toughness contribution due to the presence of the residual compressive stress in the TiN phase are summarized in Table 4. The tensile stresses generated in the ZrO_2 matrix are assumed to increase the transformability of the t-ZrO_2 phase and are incorporated in the experimentally measured composite transformability.

Crack deflection was observed to be an active toughening mechanism in all composites, as illustrated in Fig. 6. The crack deflection model of Faber and Evans[19] predicts a toughness increase of 22 up to 37% for 5 up to 50% uniformly distributed spherical secondary phase particle addition. This model has been implemented to estimate the toughness contribution from crack deflection, as summarized in Table 5. A matrix toughness of 3.3 MPa $m^{1/2}$ for non-transformable yttria-stabilized ZrO_2[20] and 2.78 MPa $m^{0.5}$ for TiN[21] was used.

The calculated toughening contribution from transformation toughening (Table 3), compressive stresses (Table 4) and crack deflection (Table 5) are superimposed on the toughness of the non-transformable and stress free composite matrix in Fig. 7. The matrix toughness is calculated according to the rule

Table 4
Compressive TiN phase stress, ZrO_2 interparticle distance and toughness contribution due to the thermal residual compressive stresses on the TiN phase for yttria stabilized ZrO_2–TiN–Al_2O_3 composites

TiN (vol%)	TiN phase stress (q) (MPa)	ZrO_2 interparticle distance (D) (μm)	ΔK_{IC} (MPa $m^{1/2}$)
35	214	1.70	0.24
40	194	1.55	0.26
50	157	1.30	0.28
60	122	1.08	0.20
70	89	0.94	0.13
80	57	0.61	0.07
90	28	0.76	0.03
95	13	0.49	0.01

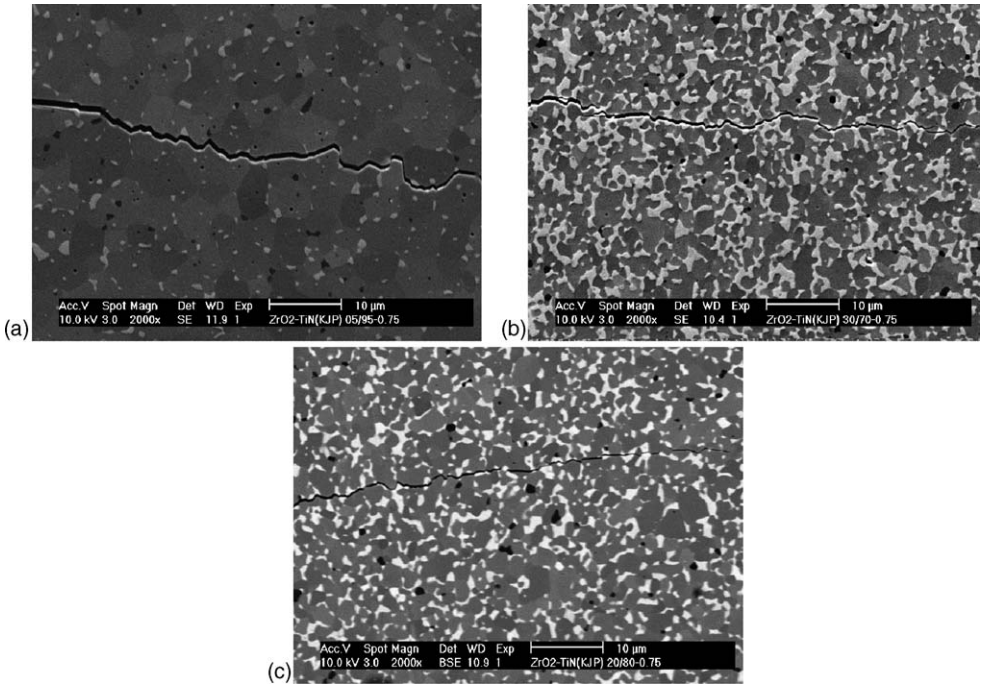

Fig. 6. Crack propagation in yttria-stabilized ZrO_2–TiN–Al_2O_3 composites with 95 (a), 70 (b) and 40 (c) vol% TiN.

Table 5
Fracture toughness calculated based on crack deflection by the secondary phase in yttria-stabilized ZrO_2–TiN–Al_2O_3 composites

TiN (vol%)	Secondary phase (vol%)	Composite/ matrix toughness ratio	Composite toughness (MPa $m^{1/2}$)	ΔK_{IC} (MPa $m^{1/2}$)
35	35	1.34	4.42	1.12
40	40	1.35	4.45	1.15
50	50	1.37	3.80	1.03
60	40	1.35	3.75	0.97
70	30	1.33	3.69	0.91
80	20	1.3	3.61	0.83
90	10	1.25	3.47	0.95
95	5	1.22	3.39	0.61

of mixtures using a toughness of 3.3 MPa $m^{1/2}$ for pure non-transformable yttria-stabilized ZrO_2[20] and 2.78 MPa.$m^{0.5}$ for TiN.[21] The calculated total toughness is found to be in good agreement with the actually measured indentation toughness, revealing that it is possible to predict the fracture toughness of the composites with good accuracy. It must be mentioned that a possible interaction between the various toughening mechanisms has not been taken into account in the analysis. Both measured and calculated fracture toughness almost decreases linearly with the TiN content.

The major toughening mechanism is transformation toughening for the composites with up to 70 vol% TiN. Crack deflection by the secondary phase is an active toughening mechanism in all composites and becomes the primary toughening mechanism in the composites with 70 up to 95 vol% TiN. The toughening contribution from the compressive stress in the TiN phase is too low to have any significant effect.

3.3. Electrical conductivity

The electrical resistivity of the composites is plotted as function of the TiN content in Fig. 8. The decrease in resistivity for the yttria-stabilized ZrO_2–TiN–Al_2O_3 composites is much sharper in the 35–50 compared to the 50–95 vol% TiN range. This can be explained by the increased connectivity and TiN grain size with increasing TiN content, as shown in Fig. 1. The

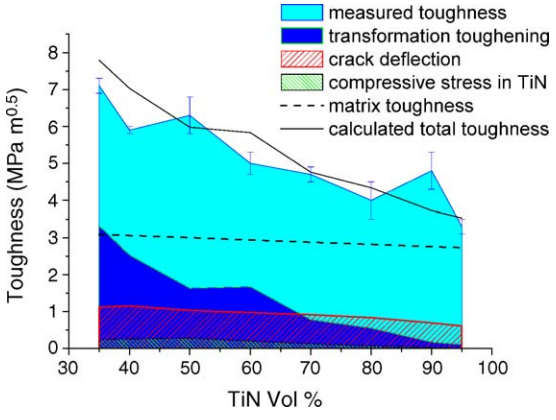

Fig. 7. Measured and calculated toughness, together with the toughness contribution of the different toughening mechanisms.

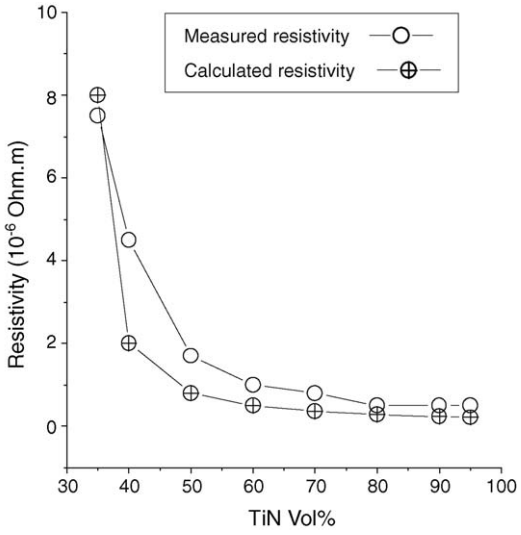

Fig. 8. Measured and calculated (Polder-Van Santen rule) electrical resistivity of yttria-stabilized ZrO_2–TiN–Al_2O_3 composites as function of the TiN content.

measured electrical conductivity was found to be in good agreement with the Polder-Van Santen mixture rule,[22] assuming a homogeneously dispersed spherical TiN secondary phase and using an electrical resisitivity of 10^9 Ωm and 20×10^{-8} Ωm for ZrO_2[14] and TiN,[16] respectively, as shown in Fig. 8. The good match between measured and calculated data confirms the validity of this assumption. At about 40 vol% TiN the composite has enough conductivity to be EDM machinable. Details about this were published in another article.[23]

4. Conclusions

Fully dense 1.75 mol% Y_2O_3 stabilized ZrO_2–TiN–Al_2O_3 composites with 0.75 wt.% Al_2O_3 and a TiN content ranging from 35–95 vol% can be achieved by hot pressing at 1550 °C for 1 h. An optimum toughness was obtained with an yttria content of 1.75 mol%.

At a constant yttria content, the hardness, fracture toughness as well as flexural strength decrease almost linearly with TiN addition. The decreasing hardness and strength can be attributed to the larger TiN grain size with increasing TiN content, whereas the reduction in toughness is due to the decreasing contribution of transformation toughening. The primary toughening mechanism of the composites with up to 70 vol% TiN is transformation toughening, whereas crack deflection is the major toughening mechanism at higher TiN contents. The contribution of the residual compressive stress in the TiN phase is negligible. As expected, the *E*-modulus increases linearly with increasing TiN content, whereas the density decreases linearly. The experimental *E*-modulus falls in-between the predictions according to the Voigt and Reuss models. The best combination of hardness, toughness and strength is obtained for the ZrO_2–TiN composites with 40 vol% TiN addition.

The electrical resistivity of the composites decreases exponentially with increasing TiN content and correlates well to the Polder-Van Santen mixture rule.

Acknowledgements

This work was performed in the framework of the MONCERAT project supported by the Commission of the European Communities within the Framework 6 Programme under project No. STRP 505541-1.

References

1. Garvie, R. C., Hannink, R. H. J. and Pascoe, R. T., Ceramic steel? *Nature*, 1975, **258**, 703–704.
2. Rühle, M. and Evans, A. G., High toughness ceramics and ceramic composites. *Prog. Mater. Sci.*, 1989, **33**, 85–167.
3. Basu, B., Vleugels, J. and Van Der Biest, O., Toughness optimisation of ZrO_2–TiB_2 composites. *Key Eng. Mater.*, 2002, **206–213**, 1177–1180.
4. Anné, G., Put, S., Vanmeensel, K., Jiang, D., Vleugels, J. and Van der Biest, O., Hard, tough and strong ZrO_2–WC composites from nanosized powders. *J. Eur. Ceram. Soc.*, 2005, **25**, 55–63.
5. Basu, B., Vleugels, J. and Van Der Biest, O., Development of ZrO_2–ZrB_2 composites. *J. Alloys Compd.*, 2002, **334**, 200–204.
6. Vleugels, J. and Van Der Biest, O., Development and characterization of Y_2O_3-stabilized ZrO_2 (Y-TZP) composites with TiB_2, TiN, TiC, and $TiC_{0.5}N_{0.5}$. *J. Am. Ceram. Soc.*, 1999, **82**(10), 2717–2720.
7. König, W., Dauw, D. F., Levy, G. and Panten, U., EDM—future steps towards the machining of ceramics. *Ann. CIRP*, 1988, **37**, 623–631.
8. Firestone, R. F., *Ceramic Applications in Manufacturing*. SME, Michigan, 1988, p. 133.
9. Anstis, G. R., Chantikul, P., Lawn, B. R. and Marshall, D. B., A critical evaluation of indentation techniques for measuring fracture toughness. *J. Am. Ceram. Soc.*, 1981, **64**, 533–538.
10. ASTM Standard E 1876-99, *Test Method for Dynamic Young's Modulus, Shear Modulus, and Poisson's Ratio for Advanced Ceramics by Impulse Excitation of Vibration*. ASTM Annual Book of Standards, Philadelphia, PA, 1994.
11. Voigt W., Über die Beziehungen den beiden Elastizitätskonstanten Isotroper Körper. *Wied Ann*. 1989, **38**, 573–87.
12. Reuss, A., Berechnung der Fliessgrenze von Mischkristallen auf Grund der Plastizitätsbedingung für Einkristalle. *Z. Angew. Math. U. Mech.*, 1929, **9**, 49–58.
13. Kral, C., Lengauer, W., Rafaja, D. and Ettmayer, P., Critical review on the elastic properties of transition metal carbides, nitrides and carbonitrides. *J. Alloys Compd.*, 1998, **265**, 215–223.
14. R. Morrell, *Handbook of Properties of Technical & Engineering Ceramics, An Introduction for Engineer and Designer (Part1)*. HSMO, London and Norwich, 1985, pp. 95–166.
15. Toraya, H., Yoshimura, M. and Somiya, S., *J. Am. Ceram. Soc.*, 1984, **67**, 119–121.
16. Pierson, H. O., *Handbook of Refractory Carbides and Nitrides. Properties, Characteristics, Processing and Applications*. Noyes Publications, Westwood, New Jersey, USA, 1996, pp. 183–187.
17. Taya, M., Hayashi, S., Kobayashi, A. and Yoon, H. S., *J. Am. Ceram. Soc.*, 1990, **73**(5), 1382–1391.
18. Mendelson, M. I., Average grain size in polycrystalline ceramics. *J. Am. Ceram. Soc.*, 1969, **52**, 443–446.
19. Faber, K. T. and Evans, A. G., Crack deflection processes. I. Theory. *Acta Metall.*, 1983, **31**, 565–576.
20. Hannink, R. H. J., Kelly, P. M. and Muddle, B. C., Transformation toughening in zirconia-containing ceramics. *J. Am. Ceram. Soc.*, 2000, **83**, 461–487.
21. Toth, L. E., *Refractory Materials, Transition Metal Carbides and Nitrides* (vol. 7). San Diego, Academic Press, 1971.
22. Polder, D. and van Santen, J. H., The effective permeability of mixtures of solids. *Physica*, 1946, **12**, 257–271.
23. Lauwers, B., Liu, W., Kruth, J. P., Vleugels, J., Jiang, D. and Van der Biest, O., Wire EDM machining of Si_3N_4 ZrO_2 and Al_2O_3-based ceramics. *Int. J. Electrical Machining*, 2005, **10**, 33–37.